A Ratiometric Sensor Based on Plant N-Terminal Degrons Able to Report Oxygen Dynamics in *Saccharomyces cerevisiae*

Mikel Lavilla Puerta [1], Vinay Shukla [1], Laura Dalle Carbonare [1], Daan A. Weits [1], Pierdomenico Perata [1], Francesco Licausi [1,2†] and Beatrice Giuntoli [1,2,†]

*1 - **Plantlab,** Institute of Life Sciences, Scuola Superiore Sant'Anna, Via Guidiccioni 8/10c, 56010 Ghezzano (PI), Italy*
*2 - **Department of Biology,** University of Pisa, Via Luca Ghini 13, 56126 Pisa, Italy*

***Correspondence to Francesco Licausi:** Plantlab, Institute of Life Sciences, Scuola Superiore Sant'Anna, Via Guidiccioni 8/10c, 56010 Ghezzano (PI), Italy. francesco.licausi@unipi.it*
https://doi.org/10.1016/j.jmb.2019.05.023

Abstract

The ability to perceive oxygen levels is crucial to many organisms because it allows discerning environments compatible with aerobic or anaerobic metabolism, as well as enabling rapid switch between these two energy strategies. Organisms from different taxa dedicate distinct mechanisms to associate oxygen fluctuations with biological responses. Following from this observation, we speculated that orthogonal oxygen sensing devices can be created by transfer of essential modules from one species to another in which they are not conserved. We expressed plant cysteine oxidase (PCOs) enzymes in *Saccharomyces cerevisiae*, to confer oxygen-conditional degradability to a bioluminescent protein tagged with the Cys-exposing N-degron typical of plant ERF-VII factors. Co-translation of a second luciferase protein, not subjected to oxygen-dependent proteolysis, made the resulting Double Luciferase Oxygen Reporter (DLOR) ratiometric. We show that DLOR acts as a proxy for oxygen dynamics in yeast cultures. Moreover, since DLOR activity was enabled by the PCO sensors, we employed this device to disclose some of their properties, such as the dispensability of nitric oxide for N-terminal cysteine oxidation and the individual performance of *Arabidopsis* PCO isoforms *in vivo*. In the future, we propose the synthetic DLOR device as a convenient, eukaryotic cell-based tool to easily screen substrates and inhibitors of cysteine oxidase enzymes *in vivo*. Replacement of the luminescent proteins with fluorescent proteins will further turn our system into a visual reporter for oxygen dynamics in living cells.

Introduction

Numerous perception mechanisms to cope with varying oxygen levels have been identified across biological kingdoms, each optimized to the ecological niche occupied and the biological process being controlled. Remarkably, transcriptional regulation of low-oxygen responses in eukaryotes converged toward a similar solution, based on proteolytic control of transcription factors by means of oxidative reactions [1]. In animal cells, the stability and activity of the transcription factor HIF-1 [2–6] iare controlled by proline and asparagine hydroxylation, catalyzed by 2-oxoglutarate and oxygen dependent hydroxylases [7,8]. The same class of enzymes is involved in controlling the half-life of sterol regulatory element binding proteins (SREBPs) [9], regulators of lipid homeostasis and metal uptake in different fungal species [10]. These ER-tethered transcription factors are tied to hypoxia by a twofold layer of regulation. In addition to direct oxidation through prolyl hydroxylases, their N-terminal fragment is endoproteolytically cleaved and released into the nucleus when sterol levels drop because of insufficient oxygen availability [11,12].

Instead, a different oxidative reaction is dedicated to oxygen-controlled gene expression in higher plants. Here, dioxygenation of amino-terminal cysteine of the group VII of the ethylene responsive factor (ERF-VII) family generates a sulfinylated residue that stimulates protein degradation *via* the 26S proteasome [13,14]. In this way, the induction of

hypoxia-responsive genes by ERF-VII is prevented under aerobic conditions. This regulation falls within a broader and interconnected sequence of post-translational modifications, defined as the N-end rule pathway [15], that dictates protein stability depending on the amino-terminal amino acid [16]. According to this pathway, N-terminal residues characterized by sulfinic and carboxylic moieties alike are substrates of arginine conjugation by Arg-transferases (ATE) [17]. This modification generates a destabilizing domain (N-degron) that can be polyubiquitinated by single subunit E3 ligase (Ub ligase N-recognin1, UBR1, in yeast) [18].

N-terminal Cys oxidation was initially assumed to occur spontaneously in the presence of oxygen and nitric oxide (NO) [19,20], leading to the designation of proteins with such N-negrons as sensors of both gaseous molecules [13,21,22]. The discovery of plant cysteine oxidases (PCOs) disclosed the possibility of enzymatic control over this step of N-end ruled proteolysis [23,24], thereby shifting the attribution of oxygen sensory function to these proteins. While oxygen represent a co-substrate for PCO activity, the contribution of NO to this process has remained more elusive, given its dispensability in *in vitro* assays but, at the same time, the stabilization of Cys-degron proteins by limiting NO accumulation *in vivo* [19,25].

Here, we describe the design of a synthetic reporter for oxygen levels, named DLOR (Dual Luciferase Oxygen Reporter), based on the plant-derived oxygen sensory pair ERF-VII/PCO and its characterization in *Saccharomyces cerevisiae*, as a proof of concept for its exploitation in orthogonal biological systems.

Results

A plant-derived reporter system expressed in yeast is autonomously controlled by oxygen

We built our investigation on the established N-degron substrate RAP2.12, an ERF-VII transcription factor from *Arabidopsis*, and the plant cysteine oxidase PCO4, shown to possess maximum activity on a RAP2.12-derived peptide *in vitro* [23]. To test whether the PCO/ERF-VII couple is sufficient to constitute a *bona fide* oxygen sensor for eukaryotic cells, we exploited *S. cerevisiae* as a biological chassis to express a ratiometric reporter for the Arg-Cys branch of the N-end rule pathway. Following the strategy devised by Bachmair and colleagues [15], we opted for a genetic fusion of two enzymes able to emit signals of easy and orthogonal detection, which are co-translationally split into single polypeptides with independent fates. We opted for a *Renilla reniformis* luciferase (Rluc) separated by means of a ubiquitin monomer from the N-degron of the RAP2.12 transcription factor, in turn fused to *Photinus pyralis* luciferase (Fluc). Ubiquitin ensures precise cleavage by deubiquitinating enzymes [26] leaving the N-terminal cysteine from the ERF-VII motif exposed [27]. The independent fate of the two cleaved modules *in vivo* could then be followed upon disruptive measurement of the two luciferase activities. We speculated that forcing oxidation of the exposed Cys in an O_2-dependent manner would conditionally channel the Fluc module toward N-end rule proteolysis and therefore named the chimeric construct as Cys-containing Double Luciferase based Oxygen Reporter (C-DLOR) (Fig. 1a). An Ala substituted version was also designed (A-DLOR), containing a C2A mutation in the $RAP_{2–28}$ peptide, which is not expected to undergo conditional proteolysis (Fig. 1a).

Coherently, with the previous report that N-terminal cysteine is not a destabilizing residue in budding yeast [28], expression of C-DLOR in MaV203 cells led to a relative luciferase activity (i.e., Fluc/Rluc ratio) of around 1 (Fig. 1b). The output of the system was not significantly modified when cells were compelled to hypoxic growth (1% O_2 v/v). Instead, concomitant expression of the *Arabidopsis thaliana* cysteine oxidase PCO4 significantly abated the relative luciferase activity (Fig. 1b). After immunoblotting of the yeast protein extracts with a Fluc antibody, we could only observe a band compatible with the DLOR cleavage product ($RAP2.12_{2–28}$-Fluc), indicating complete separation of the two luciferase modules (Supplementary Fig. 1). In this way, we made sure that the variable luminescent output reflected the activity of the $RAP2.12_{2–28}$-Fluc module, rather than that of an intact DLOR protein. The $RAP2.12_{2–28}$-Fluc protein abundance was strikingly decreased in cells expressing PCO4 under aerobic conditions, but not under hypoxia, while Rluc was unaffected by either PCO4 expression or oxygen availability (Fig. 1c and d). To make sure that DLOR dynamics were due to post-translational events, we also measured the mRNA levels of the sensor components. *Fluc* and *PCO4* transgene expression was not altered by the hypoxic treatment, whose effectiveness was verified by the induction of the hypoxia-responsive gene *CYC7* [29] (Supplementary Fig. 2a). We could therefore exclude the existence of transcriptional regulation on DLOR. Little C-DLOR residual activity was observed in PCO4-containing aerobic cells, accounting for approximately 10% of the output reached under hypoxia (Fig. 1b, e and f). Persistence of a fraction of reporter module protein could derive from excessive DLOR production, as related to PCO4 processing capacity. It is conceivable that reciprocal tuning of DLOR and PCO transcription and/or translation rates would lead to further improved dynamic range of the sensor.

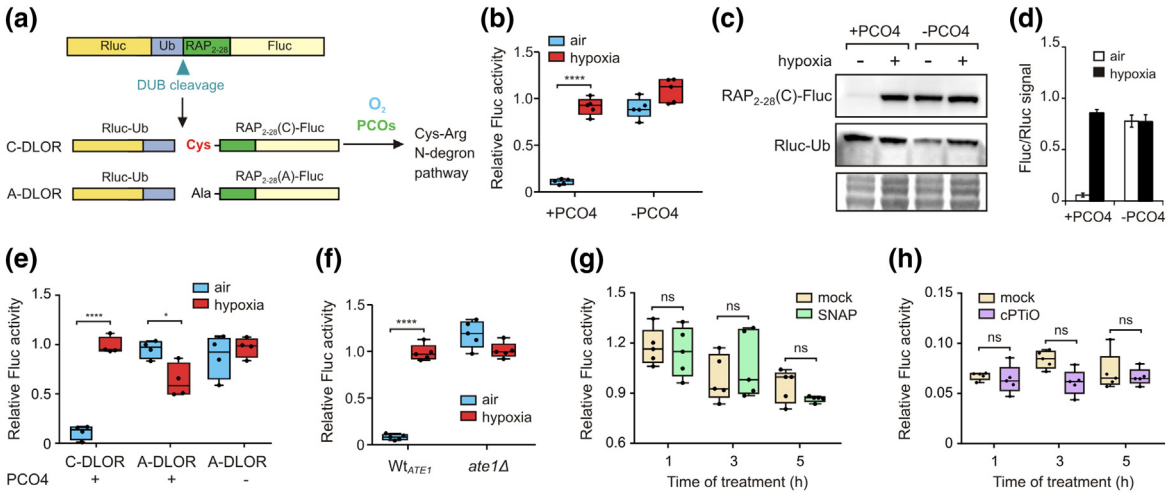

Fig. 1. The ratiometric construct DLOR reports oxygen presence in *S. cerevisiae* when co-expressed with N-terminal cysteine oxidase enzyme. (a) Design and mechanism of action of a luciferase-based oxygen reporter for yeast. (b) Relative Fluc activity (Fluc/Rluc ratio) in yeast cultures expressing C-DLOR along with the PCO4 enzyme (+PCO4) or alone (−PCO4), in hypoxia (1% O_2, 6 h) *versus* control conditions (21% O_2, 6 h). (c) Immunoblotting of RAP(C)-Fluc and Rluc-Ub abundance in the same cultures. A protein loading control is included. (d) Ratio of Fluc and Rluc protein band intensity from biological replicates shown in the immunoblots from panel c and Supplementary Fig. 1 (n = 3). (e) Relative Fluc activity in yeast cultures (n = 4) expressing PCO4 and either C-DLOR or A-DLOR under aerobic or hypoxic conditions. (f) Relative Fluc activity in wild-type or *ATE1* knock out mutant yeast expressing PCO4 and C-DLOR under aerobic or hypoxic conditions. All statistical comparisons shown between mean values indicate the level of significance after two-way ANOVA on repeated measures and Holm–Sidak test. ****$P < 0.0001$; *$0.01 \leq P < 0.05$; ns, $P > 0.05$. (g) DLOR response in yeast cells treated with 300 μM SNAP or 1% DMSO (v/v; mock), in the absence of PCO4. (h) Effect of 200 μM cPTiO or 1% DMSO (v/v, mock) on DLOR activity in yeast cells expressing PCO4. Mean values were compared by paired *t*-test at each time point; ns, non-significant difference.

Taken together, these data showed that no native PCO-like activity is encoded by the yeast genome, in agreement with the fact that no PCO-homolog could be retrieved by blast interrogation of the *S. cerevisiae* proteome (Supplementary Fig. 2b). Moreover, our results demonstrated that, once introduced in yeast, PCO4 retains the ability to restrain the abundance of Cys-exposing proteins in the presence of oxygen, compatibly with its oxygen sensing capacity. In conclusion, it can be stated that the DLOR/PCO4 pair works in an orthogonal fashion to the oxygen sensing mechanisms active in yeast to generate an oxygen-dependent output.

Regulation of DLOR activity via the N-end rule pathway

We next tested whether PCO4-induced DLOR proteolysis in *S. cerevisiae* is mediated by the N-end rule pathway. Cys substitution with Ala entirely prevented PCO4-driven reduction of reporter output under aerobic conditions (Fig. 1e), demonstrating that N-terminal Cys is required to achieve the aerobic degradation of the Fluc module. Immuno-detection displayed no major changes in the Fluc protein amount when A-DLOR was expressed in the presence of PCO4 in either ambient (21% O_2) or hypoxic (1% O_2) atmosphere (Supplementary Fig. 3a). The superior sensitivity of the dual luciferase assay also hinted at some additional oxidation-independent activity by PCO4, only achievable at low-oxygen concentrations and requiring an N-terminal alanine residue (Fig. 1e). Taken together, these results confirmed that PCO4 confers oxygen-dependent protein instability to Fluc through the Cys N-degron pathway.

Consequently, we investigated whether such regulation relies on the functionality of the Arg/N-end rule pathway. To this purpose, we targeted the genomic ATE1 locus, responsible for the N-terminal conjugation of Arg that generates a UBR1 substrate, and replaced it with a kanamycin resistance cassette (Supplementary Fig. 3b), thereby abolishing ATE1 expression (Supplementary Fig. 3c). In the mutant *ate1Δ::KanMX4* strain, C-DLOR exhibited constant activity irrespectively of the expression of PCO4 (Fig. 1f): thus, we concluded that PCO4 promotes Fluc degradation *via* the N-end rule pathway.

Despite conservation across the three eukaryotic kingdoms of ATE and UBR enzymes, and of the overall regulation of protein stability according to the N-end rule pathway [17], N-terminal cysteine does not constitute a destabilizing residue in *S. cerevisiae* [28]. It has been hypothesized that insufficient NO levels did not permit Cys oxidation in the presence of oxygen, preventing the production of the N-degron [19,30]. However, substantial NO accumulation in *S.*

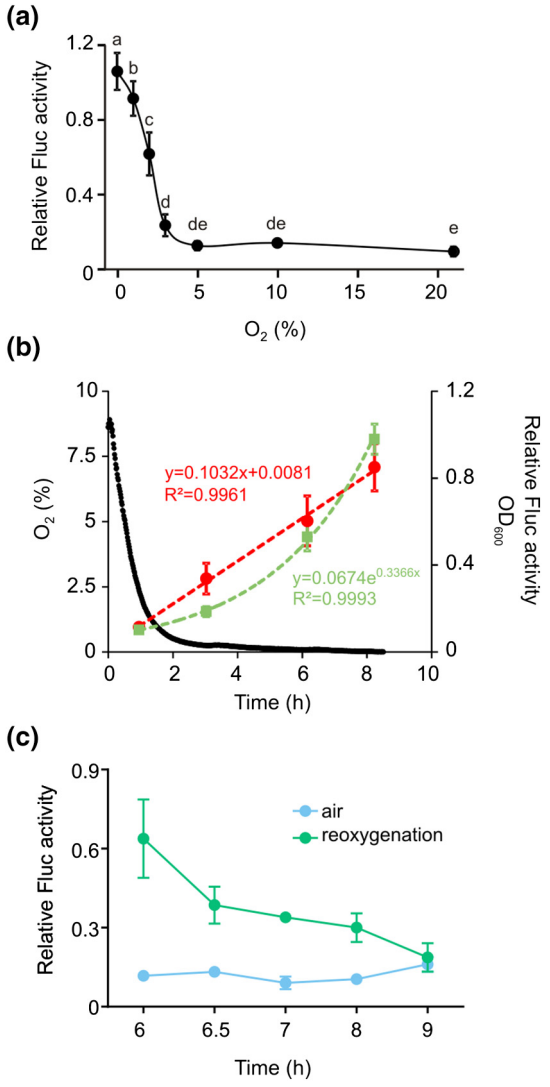

Fig. 2. DLOR responds dynamically to oxygen in the presence of PCO4. (a) DLOR activity (Fluc/Rluc ratio) in cells incubated for 6 h under different atmospheric oxygen levels (21%, 10%, 5%, 3%, 2%, 1%, or 0% O_2 v/v). Data are mean ± S.D. (n = 5). Distinct letters indicate statistically significant difference among mean values, as assessed by one-way ANOVA followed by Holm–Sidak post hoc test ($P < 0.05$). (b) Oxygen levels (black, mg l^{-1}), relative Fluc activity (red, Fluc/Rluc) and culture density (green, OD_{600}) over 6-h growth under a 1% O_2 atmosphere. Data for DLOR activity and cell density are mean ± S.D. (n = 5). Best fit regression curves are reported (dashed lines) along with their equations. Continuous oxygen measurement in the growth medium of one culture is shown at 1-min intervals. (c) DLOR activity in yeast culture shifted back to 21% O_2 after 6-h hypoxic incubation (1% O_2) (green line). Cells permanently maintained in aerobic conditions are shown as a control (cyan line). Data for DLOR activity and cell density are mean ± S.D. (n = 5).

cerevisiae has lately been detected and attributed to either NOS-like activity or nitrite reduction [31]. Moreover, PCO's need for NO to promote ERF-VII degradation in plants is still debated [23], considering that purified PCO enzymes can catalyze substrate oxidation in the absence of NO donors *in vitro* [32]. The DLOR reporter represents an ideal system to address these questions, due to its specificity for PCOs. We first tested whether the supplementation of a chemical NO donor (*S*-nitroso-*N*-acetylpenicillamine, or SNAP) was able to reduce reporter output under aerobic conditions. In the absence of PCO4, SNAP did not affect significantly C-DLOR activity (Fig. 1g). We confirmed the efficacy of the treatment by measuring the expression of copper transporter 1 (*CTR1*), an NO-induced gene [33]; *CTR1* mRNA rapidly increased upon NO stimulation, falling back to untreated levels after 5 h (Supplementary Fig. 4). We therefore concluded that absence of Cys oxidase enzymes, rather than low NO levels, excludes cysteine from the list of destabilizing residues in budding yeast. In addition, in cells expressing both transgenes, the NO scavenger 2–4-carboxyphenyl-4,4,5,5-tetramethylimidazoline-1-oxyl-3-oxide (cPTIO) did not affect PCO4-promoted DLOR instability (Fig. 1h), suggesting that PCO4 does not require NO to stimulate the degradation of protein exposing an N-terminal cysteine in living *S. cerevisiae* cells.

DLOR reports intracellular oxygen concentrations in growing yeast cultures

The results described so far prompted us to extend the characterization of the oxygen-dependent regulation imposed by PCO4, by describing DLOR activity as a function of oxygen availability. Aerobic cultures were split and incubated at different external oxygen concentrations for an equal amount of time (6 h). An atmosphere containing 3% O_2 (v/v) was able to significantly elevate DLOR signal over aerobic values, and the output rose steeply when oxygen levels were further diminished (Fig. 2a). The highest output was reached by incubation under anoxia (100% N_2 v/v) (Fig. 2a). These data indicate that, in living yeast cells, PCO4 retains full activity on the C-$RAP_{2–28}$-Fluc substrate as long as the oxygen concentration in the external atmosphere remained above 5%, while it experienced quick loss of activity below 3% O_2 (v/v).

Next, we investigated the relationship between the luminescent output and the actual oxygen concentration in the growth medium, which in turn depends on cell density, respiratory rate and atmospheric oxygen availability. To this end, DLOR activity was measured in an air-equilibrated culture stirred under 1% O_2 atmosphere and oxygen levels in the growth medium constantly monitored. In the first hour of incubation, oxygen concentration decreased down to about 2 mg l^{-1} (70 μM O_2, Fig. 2b) with no effect on DLOR activity (Supplementary Fig. 5a): this value is equivalent with the concentration of a medium

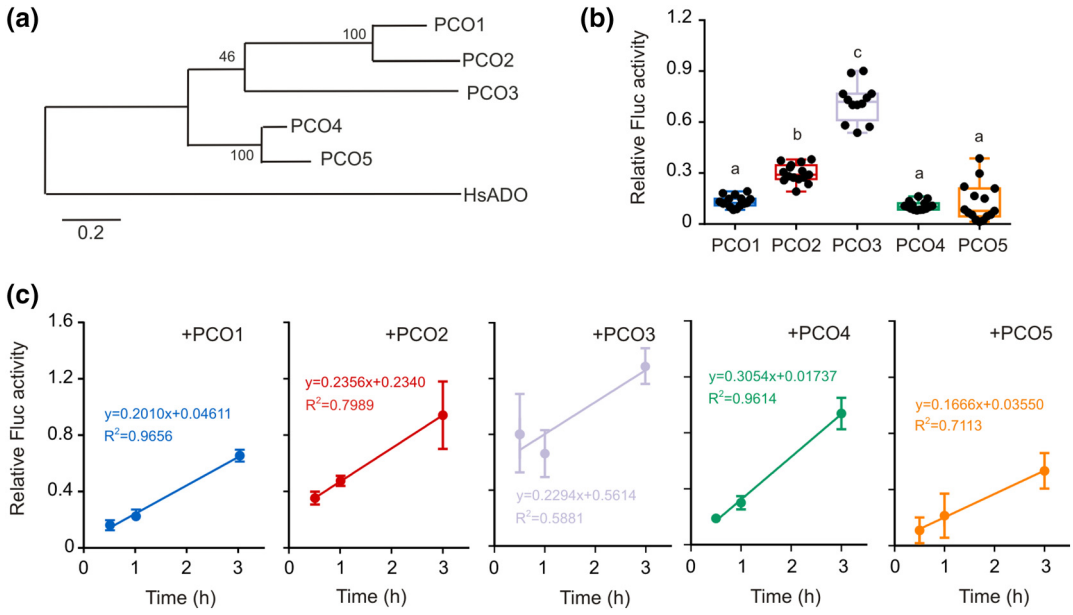

Fig. 3. *Arabidopsis* PCO isoforms impact on DLOR stability differently. (a) Phylogenetic relatedness of the five PCO family members from *Arabidopsis*. A distantly related human cysteamyl dioxygenase (ADO) was included as the root. (b) Aerobic DLOR activity (Fluc/Rluc ratio) in *S. cerevisiae* cells expressing each one of the five PCO from *Arabidopsis*. Letters indicate the statistical significance of the differences among mean values (n = 15), as assessed by one-way ANOVA followed by Holm–Sidak post hoc test ($P < 0.05$). (c) C-DLOR response to oxygen upon co-expression of different *Arabidopsis* PCOs. Data are mean ± S.D. Best-fit values for linear regressions (95% C.I.) are provided.

equilibrated with a 5% O_2 atmosphere (V/V), the response of the sensor was in agreement with previous evidence about its sensitivity (Fig. 2a). The initial decrease in dissolved oxygen was comparable in the clean medium and in the one containing cells. After 130 min, instead, the medium reached a set point of 0.6 mg l^{-1} O_2, corresponding to the equilibrium with the external 1% atmosphere, while, in the presence of exponentially growing cells, oxygen depletion slowly carried on until near-anoxia (Supplementary Fig. 5b). DLOR activation was observed at 3 h (Supplementary 5a), when oxygen concentration in the culture was 0.3 mg l^{-1} (8 μM). The luminescent output maintained a linear increase over time (Fig. 2b), while, when plotted as a function of O_2 concentration in the medium, it displayed an exponential behaviour (Supplementary Fig. 5c). Thus, with set starting OD_{600} (0.1) and external atmosphere (1% O_2), our model allows to estimate the intracellular concentration of oxygen, assumed in equilibrium with the medium, from DLOR output.

Finally, we characterized the reversibility of our synthetic system when oxygen is supplemented back. Reoxygenation elicited a faster response by DLOR than hypoxia, halving the relative signal in 1 h and restoring it back to aerobic levels in 4 h (Fig. 2c). Such a quick dynamics is compatible with active proteolysis of the Fluc reporter through the proteasome, as compared to the slower increase of the signal under hypoxia, which requires new protein synthesis.

DLOR as a tool to investigate cysteine oxidase enzyme functionality in vivo

The PCO family of *A. thaliana* comprises five members, as identified by similarity search starting from the human cysteamyl dioxygenase protein sequence (Fig. 3a). Pioneering studies by White and co-workers [32] showed that *Arabidopsis* PCO isoforms exhibit different affinity for oxygen and ERF-VII substrates *in vitro*, with PCO4 behaving as the most competent enzyme for RAP2.2 and RAP2.12 oxidation. We reasoned that the DLOR-based system provides an unprecedented way to extend the characterization of plant PCO isoforms in terms of activity in living cells. In our hands, co-expression of the dual reporter with each of the *Arabidopsis* isoforms revealed similar output levels for PCO1, PCO4 and PCO5 under aerobic conditions, whereas DLOR activity was higher in PCO2 and PCO3 expressing cells (Fig. 3b). To investigate whether these differences could be ascribed to the oxygen sensitivity of the PCO isoforms or rather to their different turnover, we generated GFP-tagged versions of all five PCOs and expressed them in yeast with the C-DLOR construct. First, we tested whether the GFP fusion affected the enzyme activity

in air and hypoxia using PCO4 as an example over the same time-course described above, obtaining comparable patterns of relative luminescence (Supplementary Fig. 6a). Next, we assessed PCO protein levels, by immunoblotting, along with dual luciferase activity in log-phase cultures. Six-hour growth was necessary to obtain a sufficient amount of cell extracts for immunoblotting from the same culture volume used before. We did not observe substantial changes in the abundance of GFP-PCO1, 4 and 5 when comparing aerobic and hypoxic samples, while PCO2 and 3 displayed higher degree of variability across the biological replicates (Supplementary Fig. 6b). Moreover, the activity of GFP-tagged versions on the DLOR response did not significantly differ from that of the untagged ones (Supplementary Fig. 6c). Based on these data, we focused on PCO1, 4 and 5, assuming that their turnover is not affected by hypoxia. Among these three isoforms, linear regressions modeling of the hypoxic patterns indicated stronger hypoxia responsiveness for PCO4, which released the inhibition significantly faster than PCO1 and PCO5 after the onset of 1% O_2 hypoxia (Fig. 3c and Supplementary Table 1).

Discussion

With the introduction of the DLOR/PCO couple in budding yeast, we proved that the Arg-Cys N-end rule pathway acts as a genuine oxygen perception mechanism. In plants, it has been proposed that other regulatory mechanisms might be required upstream of PCO to rapidly activate ERF-VII under hypoxia. Instead, the experiments reported here support the primary role of PCOs in inhibiting ERF-VII activity in an oxygen-dependent manner, similar to what prolyl hydroxylases do to the HIF1 transcription factor in animals [3]. First, we obtained evidence that in yeast cysteine acts as a conditional degradation tag exclusively when it is oxidized by PCO (Fig. 1b and c). Thus, spontaneous oxidation in our eukaryotic host system was ruled out. Our results prove that fungal cells possess all requirements for oxygen-dependent proteolysis of Cys-exposing peptides except for N-terminal Cys oxidases, providing a likely explanation to the notion of Cys not being a destabilizing residue in wild type yeast. Moreover, we showed that, once isolated from their original plant background, PCOs still serve as oxygen sensors. In plants, hypothetical upstream regulatory mechanisms have been proposed to link PCO activity to oxygen. However, conservation of such mechanisms is unlikely in yeast, where no PCO homolog is present. In addition, oxygen-independent inhibition of PCO activity by iron starvation or zinc excess also causes a hypoxia-like transcriptional response [34]. Considered together, these observations seem to entail that cysteine oxidases act as direct switches for oxygen also in plants. The recent reports of Cys N-degron substrates, not limited to the ERF-VIIs, driving plant development also favor a main role for PCOs in driving adaptation to cellular oxygen availability [35–38]. Nonetheless, this does not exclude the possibility that additional indirect acute hypoxia sensing mechanisms operate aside PCO in plants. For instance, energy-dependent regulation of ERF-VII localization through changes in the cellular acyl-CoA pool has been demonstrated in *Arabidopsis* [39]. Moreover, it has been proposed that reactive oxygen species caused by an impaired mitochondrial electron transport could regulate membrane channels and trigger secondary signaling [40].

The involvement of NO in the processing of Cys/N-end rule substrates is still matter of investigation. An *in vitro* arginylation assay on a Cys-starting RGS4 peptide has proven sensitive to the presence of NO donors [19], leading to the conclusion that Cys oxidation could be spontaneous and dependent on the concomitant presence of NO. Opposite to it, other assays indicate that the oxidation and arginylation of RAP2.12-derived N-termini can take place in a reaction environment completely devoid of NO, when PCO and oxygen are provided [26]. In plants, NO promotes instability of some Cys-starting proteins and thus has been hypothesized as a requisite for the PCO-catalyzed oxidation of N-terminal cysteine *in vivo* [22,26,29]. In our *in vivo* assay, we observed that PCO4 could promote the turnover of the reporter independently of NO (Fig. 1g and Supplementary Fig. 4). As we demonstrated that DLOR is able to recapitulate PCO activity in a heterologous system, our data suggest that in plants NO is rather likely to act in parallel to thiol oxidase enzymes to modulate the stability of Cys/N-end rule substrates.

The approach to generate a genetically encoded oxygen sensor is specular to the one recently attempted by us for plant cells, where we exploited the animal hypoxia signaling pathway [41]. In both systems, the output relies on long-lived luciferase enzymes. Their replacement with variants with fast turnover will be instrumental to trigger a prompter DLOR response to oxygen dynamics. Furthermore, the same ratiometric strategy adopted in the design of the sensor described here might be exploited for the design of a visual reporter of oxygen. Substitution of the luciferase modules with short-lived fluorescent proteins (e.g., fast-turning GFP and RFP versions) would easily turn the disruptive DLOR sensor into a dynamic reporter for oxygen in live cells. Nevertheless, in its present form, DLOR can already be proposed as a suitable system for the identification of inhibitors of terminal cysteine oxidases. In the same way, we envision to employ it in the screening of novel substrates to expand the set of proteins subjected to the Arg-Cys branch of the N-end rule pathway.

Materials and Methods

Yeast strains

The haploid *S. cerevisiae* MaV203 strain (*MATα; leu2–3112; trp1–901; his3Δ200; ade2–101; cyh2^R; can1^R; gal4Δ; gal80Δ; GAL1::lacZ; HIS3$_{UASGAL1}$::HIS3@LYS2; SPAL10::URA3*) was purchased from Thermo-Fisher Scientific. *S. cerevisiae ate1Δ::KanMX4* strain was generated from haploid yeast (MaV203) by homologous recombination following the protocol described by Gardner and Jaspersen [42]. A synthetic ate1Δ::KanMX4 homology repair cassette [43] was used that contained 60-nucleotide homology arms with the 5′ and 3′ genomic regions flanking the coding sequence of the Saccharomyces *ATE1* gene (Supplementary Fig. 2b).

Yeast culture

S. cerevisiae colonies were grown at 30 °C in liquid yeast synthetic medium, containing 6.7 g l^{-1} Yeast Nitrogen Base (DIFCO), 1.37 g l^{-1} Yeast Dropout Medium (Sigma-Aldrich) and 20 g l^{-1} glucose, plus suitable supplements (0.16 M uracil, 0.8 M histidine–HCl, 0.8 M leucine and 0.32 M tryptophan when complete). Overnight cultures were diluted to OD_{600} 0.1 (for treatments up to 6 h long) or 0.05 (for treatments longer than 6 h) in 50-ml Falcon tubes and grown at 150 rpm for the duration of the treatments at 30 °C. In all cases, the duration of the treatments never exceeded the time span associated with the exponential growth phase. At the end of the treatments, cells were collected by centrifugation for subsequent gene expression analyses, protein immunoblotting and luciferase activity assays. In case of growth on plates, media were supplemented with 20 g l^{-1} micro-agar (Sigma-Aldrich).

Production of yeast expression plasmids

All PCR amplifications were carried out using Phusion polymerase (Thermo-Fisher Scientific). Expression plasmids were propagated in Mach1 *Escherichia coli* cells (Thermo Fisher Scientific). DLOR constructs were obtained by gene synthesis by GeneArt (Thermo Fisher Scientific). The full C-DLOR cassette (RLuc–UBQ–RAP$_{2–28}$–Fluc) was ligated into pENTR™/D-TOPO® (Thermo Fisher Scientific). The resulting entry plasmid was exploited as a template for site-directed mutagenesis of the Cys-encoding triplet (TGT) into an Ala-encoding one (GCT), using DLOR_CtoAFw and DLOR_CtoARv primers (Supplementary Table 2), to obtain the A-DLOR entry plasmid. Both DLOR constructs were recombined into the integrative vector pAG304GPD-ccdB (Addgene plasmid no. 14136) with the Gateway LR Clonase II Enzyme mix (Thermo Fisher Scientific), to drive DLOR expression under control of the glyceraldehyde-3-phosphate dehydrogenase (*GAP*) promoter.

The coding sequences of the five *PCO* genes were amplified from *Arabidopsis* cDNA, retro-transcribed by means of the Maxima First Strand cDNA Synthesis Kit (Thermo Fisher Scientific), using the specific primers described in Supplementary Table S2 and cloned into pENTR™/D-TOPO®. The PCO containing entry plasmids were recombined into the pAG415GPD-ccdB vector (Addgene plasmid no. 14146), to direct their constitutive expression under control of the *GAP* promoter. The GFP-tagged versions were generated by recombination in the pAG415GPD-EGFP-ccdB destination vector (Addgene plasmid no. 14314).

Yeast transformation

Yeast competent cells were produced and transformed with the FCC-LiAc method, following the protocol described by Gietz and Schiestl [44]. pAG304GPD-DLOR and pAG304GPD-ccdB plasmids were linearized with BstXI (Thermo Fisher Scientific) prior to transformation. Colonies bearing the recombined pAG304GPD-DLOR and pAG415GPD-PCO plasmids, or the empty (unrecombined) plasmids used as negative controls, were selected based on auxotrophy complementation, on tryptophan- or leucine-defective plates, respectively. A synthetic ate1Δ::KanMX4 sequence (Gene Art; Supplementary File 1) was amplified with primers ate1Δ::KanMX4Fw and ate1Δ::KanMX4Rv. Once purified, the PCR product was directly delivered to competent MaV203 bearing the pAG304GPD-DLOR and pAG415GPD-PCO constructs, according to Gietz and Schiestl [44]. Recombinants were selected on plates containing 300 μM G418 (Sigma-Aldrich) and lacking tryptophan and leucine.

Low-oxygen treatments

Air-equilibrated cultures from overnight growth were diluted to OD_{600} = 0.1 and moved to hypoxic growth conditions into a Gloveless Anaerobic chamber (COY), or returned to the original incubator in the case of aerobic control cultures. The built-in gas mixing system was exploited to reach the desired oxygen concentration in the internal environment of the anaerobic chamber, upon blending of nitrogen gas with atmospheric air. Constant temperature of 30 °C and shaking of 150 rpm were maintained along all treatments, which were protracted for the time specified in each experiment. Repeated samplings from the same culture were carried out in time-course experiments.

Chemical treatments

SNAP (300 μM; Sigma-Aldrich) or 200 μM cPTiO (2–4-carboxyphenyl-4,4,5,5-tetramethylimidazoline-

1-oxyl-3-oxide; Sigma-Aldrich) in 0.1% DMSO (v/v) was applied to growing yeast cultures at OD_{600} = 0.1. Mock-treated cultures were supplemented with 0.1% DMSO (v/v). Treatments were protracted for the specified time.

Measurement of relative luciferase activity

Luciferase activity was quantified from 50 µl yeast culture using the Dual-Luciferase® Reporter (DLR™) Assay System (Promega). Cells grown as described in the section "Yeast culture" were recovered by centrifugation and pellets were lysed in 50 µl 1 × Passive Lysis Buffer. Luciferase activities measured according to the manufacturer's protocols, using a Lumat LB 9507 Tube Luminometer (Berthold). Data were expressed as Fluc/Rluc signal ratio ("relative Fluc activity").

Immunoblotting

Total *S. cerevisiae* proteins were extracted following von der Haar [45]. In brief, cells were incubated in 100 mM NaOH, 50 mM EDTA and 2% SDS at 90 °C for 10 min before adding acetic acid to a final concentration of 100 mM. Samples were incubated as described above and spun at top speed to remove cell debris. Soluble protein extract was denatured, loaded on polyacrylamide gels (NuPage Bis-Tris Gels, Thermo Fisher Scientific) and separated *via* SDS-PAGE. Proteins were transferred on a polyvinylidene difluoride membrane (Bio-Rad) using the TransBlot® Turbo transfer system (Bio-Rad). To obtain a positive control for the DLOR modules, a wheat germ extract expressing the construct was loaded along with the yeast cell lysates. To this end, the construct was cloned in the pF3A WG (BYDV) Flexi® Vector (Promega), and the resulting expression vector was transcribed and translated *in vitro* with the TnT® Coupled Wheat Germ Extract Systems (Promega), following the manufacturer's recommendations.

For the immunodetection, a polyclonal anti-Fluc (G7451, Promega, used at 1000-fold dilution), a monoclonal anti-Rluc (MAB4410, Millipore, used at 1000 fold dilution) and a monoclonal anti-GFP antibody (11814460001, Roche, used at 2000 fold dilution) were diluted in 4% skim milk solution in PBST to detect firefly luciferase, renilla luciferase and GFP, respectively. Secondary anti-mouse IgG HRP-conjugated (BioVision, cat. no. 6402-05) was used to detect renilla luciferase and GFP, anti-Rabbit IgG HRP-conjugated (AS09 602, Agrisera, 1:10000) for firefly luciferase. The detection was carried out by means of the SuperSignal™ West Dura (Thermo Fisher Scientific). Protein loading on the gels was evaluated by membrane staining with 0.1% amido black 10-B, in 45% methanol and 10% acetic acid, followed by decoloration in 90% methanol and 2% acetic acid. Signal detection took place in a ChemiDoc™ MP Imaging System (Bio-Rad). Blots are representative images following the analysis of four independent clones of each genotype.

Gene expression analyses

Yeast total RNA isolation was carried out as described by Schmitt *et al*. [46] with minor modifications. *S. cerevisiae* cells were resuspended in 50 mM sodium acetate, 10 mM EDTA and 1% SDS. An equal amount of phenol was added to the cell suspension. Samples were vortexed and incubated at 65 °C for 4 min first, and then at −20 °C for 15 min, before centrifugation at top speed for 2 min. The aqueous phase was recovered and subjected to sequential phenol:chloroform:isoamyl alcohol (25:24:1) and chloroform phase extraction. Finally, nucleic acids were precipitated by centrifugation from the aqueous phase, using 2 volumes of ice-cold absolute ethanol supplemented with sodium acetate at a final concentration of 300 mM. Pellets were resuspended in RNAse-free water. RNA concentration was measured using a µodrop plate reader (Thermo Fisher Scientific), and its quality was checked by electrophoresis in 1% agarose gels. Total RNA was then processed with Maxima cDNA synthesis kit (Thermo Fisher Scientific) using 1 µg total RNA, according to the manufacturer's protocol. Gene expression levels were assessed by Real-Time qPCR, using the PowerUp SYBR® Green Master Mix (Thermo Fisher Scientific) and a 7300 Real Time PCR System (Applied Biosystems). Gene-specific primers and their sequences are listed in Supplementary Table 2. Relative gene expression was calculated according to the ΔΔCt method [47], using *Actin 1* as the housekeeping gene.

Oxygen concentration measurements

Oxygen levels were assessed live in the sterile yeast growth medium and in the medium containing a growing yeast suspension, in separate experiments. Oxygen concentration was measured with a phosphorescent sensor (Firesting O_2 Optical Oxygen Meter, Pyroscience). An oxygen sensing spot was attached to the inner surface of the 50-ml tube used, in contact with the growing yeast culture or with the clean medium. A SPADBAS adapter held the contactless sensor to the outside of the tube. Record of the inner temperature was kept in a separate tube. Data were recorded using the Oxygen Logger software.

Statistical analysis

Cultures were started from five independent yeast colonies for each experimental thesis, unless differently stated. Analyses were carried our using

GraphPad Prism version 6.01 for Windows (GraphPad Software, La Jolla, CA, USA; www.graphpad.com). Statistical significance of mean differences was assessed by two-way ANOVA on repeated measurements, followed by the Holm–Sidak multiple comparison test. To evaluate the effect of SNAP and cPTiO on DLOR activity over time, an ANOVA on repeated measurements was carried out. Box plots represent median (line) and interquartile range, and whiskers span from minimum to maximum values.

CRediT authorship contribution statement

Mikel Lavilla Puerta: conceptualization, data curation, formal analysis, investigation, methodology. **Vinay Shukla:** Sinvestigation, methodology, formal analysis. **Laura Dalle Carbonare:** methodology. **Daan A. Weits:** methodology, data curation. **Pierdomenico Perata:** funding acquisition. **Francesco Licausi:** project administration,supervision, writing original draft, writing review & editing, conceptualization, data curation, formal analysis. **Beatrice Giuntoli:** project administration, supervision, writing original draft, writing review & editing, conceptualization, data curation, formal analysis, investigation.

Acknowledgments

We are grateful to Alvaro Galli and Arianna Tavanti for discussion and advices about yeast growth and genetic manipulation. This study was financially supported by the Scuola Superiore Sant'Anna and the University of Pisa.

Conflict of Interest Statement: All authors declare the absence of any conflict of interest and any awarded or filed patents pertaining to the results presented in the paper.

Data and Materials Availability: Plasmids for yeast transformation were purchased at the Addgene repository, upon signature of the due MTA documents.

Appendix A. Supplementary data

Supplementary data to this article can be found online at https://doi.org/10.1016/j.jmb.2019.05.023.

Received 13 January 2019;
Received in revised form 10 May 2019;
Available online 22 May 2019

Keywords:
N-end rule pathway;
plant cysteine oxidase;
synthetic biology;
Saccharomyces cerevisiae

†Senior authors.

Abbreviations used:
cPTIO, 2-(4-carboxyphenyl)-4,4,5,5-tetramethylimidazolinone-1-oxyl-3-oxide; ERF-VII, ethylene response factor VII; PCO, plant cysteine oxidase; SNAP, *S*-nitroso-*N*-acetylpenicillamine.

References

[1] J.T. van Dongen, F. Licausi, Oxygen sensing and signaling, Annu. Rev. Plant Biol. (2015) https://doi.org/10.1146/annurev-arplant-043014-114813.

[2] N. Masson, C. Willam, P.H. Maxwell, C.W. Pugh, P.J. Ratcliffe, Independent function of two destruction domains in hypoxia-inducible factor-?? chains activated by prolyl hydroxylation, EMBO J (2001) https://doi.org/10.1093/emboj/20.18.5197.

[3] P. Jaakkola, D.R. Mole, Y.-M. Tian, M.I. Wilson, J. Gielbert, S.J. Gaskell, et al, Targeting of HIF-alpha to the von Hippel–Lindau ubiquitylation complex by O2-regulated prolyl hydroxylation, Science (80-.). 292 (2001) 468–472. https://doi.org/10.1126/science.1059796.

[4] G.L. Wang, B.H. Jiang, E.A. Rue, G.L. Semenza, Hypoxia-inducible factor 1 is a basic-helix-loop-helix-PAS heterodimer regulated by cellular O2 tension, Proc. Natl. Acad. Sci. 92 (1995) 5510–5514, https://doi.org/10.1073/pnas.92.12.5510.

[5] G.L. Semenza, G.L. Wang, A nuclear factor induced by hypoxia via de novo protein synthesis binds to the human erythropoietin gene enhancer at a site required for transcriptional activation, Mol. Cell. Biol. (1992) https://doi.org/10.1128/MCB.12.12.5447.

[6] A.C.R. Epstein, J.M. Gleadle, L.A. McNeill, K.S. Hewitson, J. O'Rourke, D.R. Mole, M. Mukherji, E. Metzen, M.I. Wilson, A. Dhanda, Y.M. Tian, N. Masson, D.L. Hamilton, P. Jaakkola, R. Barstead, J. Hodgkin, P.H. Maxwell, C.W. Pugh, C.J. Schofield, P.J. Ratcliffe, *C. elegans* EGL-9 and mammalian homologs define a family of dioxygenases that regulate HIF by prolyl hydroxylation, Cell. 107 (2001) 43–54. https://doi.org/10.1016/S0092-8674(01)00507-4.

[7] D. Lando, D.J. Peet, J.J. Gorman, D.A. Whelan, M.L. Whitelaw, R.K. Bruick, FIH-1 is an asparaginyl hydroxylase enzyme that regulates the transcriptional activity of hypoxia-inducible factor, Genes Dev. 16 (2002) 1466–1471, https://doi.org/10.1101/gad.991402.

[8] R.J. Appelhoffl, Y.M. Tian, R.R. Raval, H. Turley, A.L. Harris, C.W. Pugh, P.J. Ratcliffe, J.M. Gleadle, Differential function of the prolyl hydroxylases PHD1, PHD2, and PHD3 in the regulation of hypoxia-inducible factor, J. Biol. Chem. 279 (2004) 38458–38465, https://doi.org/10.1074/jbc.M406026200.

[9] C.Y.S. Lee, T.L. Yeh, B.T. Hughes, P.J. Espenshade, Regulation of the Sre1 hypoxic transcription factor by oxygen-dependent control of DNA binding, Mol. Cell (2011) https://doi.org/10.1016/j.molcel.2011.08.031.

[10] N. Grahl, K.M. Shepardson, D. Chung, R.A. Cramer, Hypoxia and fungal pathogenesis: to air or not to air? Eukaryot Cell (2012) https://doi.org/10.1128/EC.00031-12.

[11] C.M. Bien, P.J. Espenshade, Sterol regulatory element binding proteins in fungi: hypoxic transcription factors linked to pathogenesis, Eukaryot. Cell (2010) https://doi.org/10.1128/EC.00358-09.

[12] A.L. Hughes, B.L. Todd, P.J. Espenshade, SREBP pathway responds to sterols and functions as an oxygen sensor in fission yeast, Cell (2005) https://doi.org/10.1016/j.cell.2005.01.012.

[13] F. Licausi, M. Kosmacz, D.A. Weits, B. Giuntoli, F.M. Giorgi, L.A.C.J. Voesenek, P. Perata, J.T. Van Dongen, Oxygen sensing in plants is mediated by an N-end rule pathway for protein destabilization, Nature (2011) https://doi.org/10.1038/nature10536.

[14] D.J. Gibbs, S.C. Lee, N. Md Isa, S. Gramuglia, T. Fukao, G. W. Bassel, C.S. Correia, F. Corbineau, F.L. Theodoulou, J. Bailey-Serres, M.J. Holdsworth, Homeostatic response to hypoxia is regulated by the N-end rule pathway in plants, Nature (2011) https://doi.org/10.1038/nature10534.

[15] A. Bachmair, D. Finley, A. Varshavsky, In vivo half-life of a protein is a function of its amino-terminal residue, Science (80-.). (1986). https://doi.org/10.1126/science.3018930.

[16] A. Varshavsky, The N-end rule pathway and regulation by proteolysis., Protein Sci. (2011). https://doi.org/10.1002/pro.666.

[17] T. Tasaki, S.M. Sriram, K.S. Park, Y.T. Kwon, The N-end rule pathway., Annu. Rev. Biochem. 81 (2012) 261–89. https://doi.org/10.1146/annurev-biochem-051710-093308.

[18] Z. Xia, A. Webster, F. Du, K. Piatkov, M. Ghislain, A. Varshavsky, Substrate-binding sites of UBR1, the ubiquitin ligase of the N-end rule pathway, J. Biol. Chem. (2008) https://doi.org/10.1074/jbc.M802583200.

[19] R.G. Hu, J. Sheng, X. Qi, Z. Xu, T.T. Takahashi, A. Varshavsky, The N-end rule pathway as a nitric oxide sensor controlling the levels of multiple regulators, Nature (2005) https://doi.org/10.1038/nature04027.

[20] M.J. Lee, T. Tasaki, K. Moroi, J.Y. An, S. Kimura, I.V. Davydov, Y.T. Kwon, RGS4 and RGS5 are in vivo substrates of the N-end rule pathway, Proc. Natl. Acad. Sci. (2005) https://doi.org/10.1073/pnas.0507533102.

[21] D.J. Gibbs, N. Mdlsa, M. Movahedi, J. Lozano-Juste, G.M. Mendiondo, S. Berckhan, N. Marín-delaRosa, J. VicenteConde, C. SousaCorreia, S.P. Pearce, G.W. Bassel, B. Hamali, P. Talloji, D.F.A. Tomé, A. Coego, J. Beynon, D. Alabadí, A. Bachmair, J. León, J.E. Gray, F.L. Theodoulou, M.J. Holdsworth, Nitric oxide sensing in plants is mediated by proteolytic control of group VII ERF transcription factors, Mol. Cell (2014) https://doi.org/10.1016/j.molcel.2013.12.020.

[22] J. Vicente, G.M. Mendiondo, M. Movahedi, M. Peirats-Llobet, Y. Ting Juan, et al, The Cys-Arg/N-end rule pathway is a general sensor of abiotic stress in flowering plants, Curr. Biol. 27 (2017) 3183–3190.e4. https://doi.org/10.1016/j.cub.2017.09.006.

[23] M.D. White, M. Klecker, R.J. Hopkinson, D.A. Weits, C. Mueller, C. Naumann, R. O'Neill, J. Wickens, J. Yang, J.C. Brooks-Bartlett, E.F. Garman, T.N. Grossmann, N. Dissmeyer, E. Flashman, Plant cysteine oxidases are dioxygenases that directly enable arginyl transferase-catalysed arginylation of N-end rule targets, Nat. Commun. 8 (2017). https://doi.org/10.1038/ncomms14690.

[24] D.A. Weits, B. Giuntoli, M. Kosmacz, S. Parlanti, H.M. Hubberten, H. Riegler, R. Hoefgen, P. Perata, J.T. Van Dongen, F. Licausi, Plant cysteine oxidases control the oxygen-dependent branch of the N-end-rule pathway, Nat. Commun. (2014) https://doi.org/10.1038/ncomms4425.

[25] D.J. Gibbs, J. Bacardit, A. Bachmair, M.J. Holdsworth, The eukaryotic N-end rule pathway: conserved mechanisms and diverse functions, Trends Cell Biol. 24 (2014) 603–611, https://doi.org/10.1016/j.tcb.2014.05.001.

[26] C.P. Grou, M.P. Pinto, A.V. Mendes, P. Domingues, J.E. Azevedo, The de novo synthesis of ubiquitin: identification of deubiquitinases acting on ubiquitin precursors, Sci. Rep. (2015) https://doi.org/10.1038/srep12836.

[27] J. Bailey-Serres, T. Fukao, D.J. Gibbs, M.J. Holdsworth, S.C. Lee, F. Licausi, P. Perata, Making sense of low oxygen sensing, Trends Plant Sci. 17 (2012) 129–138. https://doi.org/10.1016/j.tplants.2011.12.004.

[28] E. Graciet, F. Mesiti, F. Wellmer, Structure and evolutionary conservation of the plant N-end rule pathway, Plant J (2010) https://doi.org/10.1111/j.1365-313X.2009.04099.x.

[29] K.E. Kwast, P.V. Burke, B.T. Staahl, R.O. Poyton, Oxygen sensing in yeast: evidence for the involvement of the respiratory chain in regulating the transcription of a subset of hypoxic genes, Proc. Natl. Acad. Sci. U. S. A. (1999) https://doi.org/10.1073/PNAS.96.10.5446.

[30] R.G. Hu, C.S. Brower, H. Wang, I.V. Davydov, J. Sheng, J. Zhou, T.K. Yong, A. Varshavsky, Arginyltransferase, its specificity, putative substrates, bidirectional promoter, and splicing-derived isoforms, J. Biol. Chem. (2006) https://doi.org/10.1074/jbc.M604355200.

[31] R.I. Astuti, R. Nasuno, H. Takagi, Nitric oxide signalling in yeast, Adv. Microb. Physiol. (2018) https://doi.org/10.1016/bs.ampbs.2018.01.003.

[32] M.D. White, J.J.A.G. Kamps, S. East, L.J. Taylor Kearney, E. Flashman, The plant cysteine oxidases from *Arabidopsis thaliana* are kinetically tailored to act as oxygen sensors, J. Biol. Chem. 293 (2018) 11786–11795, https://doi.org/10.1074/jbc.RA118.003496.

[33] R. Nasuno, M. Aitoku, Y. Manago, A. Nishimura, Y. Sasano, H. Takagi, Nitric oxide-mediated antioxidative mechanism in yeast through the activation of the transcription factor Mac1, PLoS One (2014) https://doi.org/10.1371/journal.pone.0113788.

[34] L. Dalle Carbonare, M. White, V. Shukla, A. Francini, P. Perata, E. Flashman, L. Sebastiani, F. Licausi, Zinc excess induces a hypoxia-like response by inhibiting cysteine oxidases in poplar roots, Plant Physiol. (2019) pp.01458.2018. https://doi.org/10.1104/pp.18.01458.

[35] V. Shukla, L. Lombardi, S. Iacopino, A. Pencik, O. Novak, P. Perata, B. Giuntoli, F. Licausi, Endogenous hypoxia in lateral root primordia controls root architecture by antagonizing auxin signaling in *Arabidopsis*, Mol. Plant (2019) https://doi.org/10.1016/j.molp.2019.01.007.

[36] M. Abbas, S. Berckhan, D.J. Rooney, D.J. Gibbs, J. Vicente Conde, C. Sousa Correia, G.W. Bassel, N. Marín-De La Rosa, J. León, D. Alabadí, M.A. Blázquez, M.J. Holdsworth, Oxygen sensing coordinates photomorphogenesis to facilitate seedling survival, Curr. Biol. 25 (2015) 1483–1488, https://doi.org/10.1016/j.cub.2015.03.060.

[37] D.J. Gibbs, H.M. Tedds, A.M. Labandera, M. Bailey, M.D. White, S. Hartman, C. Sprigg, S.L. Mogg, R. Osborne, C. Dambire, T. Boeckx, Z. Paling, L.A.C.J. Voesenek, E. Flashman, M.J. Holdsworth, Oxygen-dependent proteolysis regulates the stability of angiosperm polycomb repressive complex 2 subunit VERNALIZATION 2, Nat. Commun. (2018) https://doi.org/10.1038/s41467-018-07875-7.

[38] D.A. Weits, N.C.W. Kunkowska, A.B. Kamps, K. Portz, Z. Packbier, N.K. Nemec-Venza, et al, An apical hypoxic niche sets the pace over shoot meristem activity, Nature. (n.d.).

[39] R.R. Schmidt, M. Fulda, M.V. Paul, M. Anders, F. Plum, D.A. Weits, et al, Low-oxygen response is triggered by an ATP-

dependent shift in oleoyl-CoA in *Arabidopsis* Proc. Natl. Acad. Sci. 115 (2018) E12101 LP-E12110. https://doi.org/10.1073/pnas.1809429115.

[40] F. Wang, Z.H. Chen, S. Shabala, Hypoxia sensing in plants: on a quest for ion channels as putative oxygen sensors, Plant Cell Physiol (2017) https://doi.org/10.1093/pcp/pcx079.

[41] S. Iacopino, S. Jurinovich, L. Cupellini, L. Piccinini, F. Cardarelli, P. Perata, B. Mennucci, B. Giuntoli, F. Licausi, A synthetic oxygen sensor for plants based on animal hypoxia signalling, Plant Physiol (2019)https://doi.org/10.1104/pp.18.01003.

[42] J.M. Gardner, S.L. Jaspersen, Manipulating the yeast genome: deletion, mutation, and tagging by PCR, Methods Mol. Biol. 1205 (2014) 45–78, https://doi.org/10.1007/978-1-4939-1363-3_5.

[43] A. Wach, A. Brachat, R. Pöhlmann, P. Philippsen, New heterologous modules for classical or PCR-based gene disruptions in *Saccharomyces cerevisiae*, Yeast. 10 (1994) 1793–1808, https://doi.org/10.1002/yea.320101310.

[44] R.D. Gietz, R.H. Schiestl, Frozen competent yeast cells that can be transformed with high efficiency using the LiAc/SS carrier DNA/PEG method, Nat. Protoc. 2 (2007) 1–4, https://doi.org/10.1038/nprot.2007.17.

[45] T. von der Haar, Optimized protein extraction for quantitative proteomics of yeasts, PLoS One. 2 (2007). doi:https://doi.org/10.1371/journal.pone.0001078.

[46] M.E. Schmitt, T.A. Brown, B.L. Trumpower, A rapid and simple method for preparation of RNA from *Saccharomyces cerevisiae*, Nucleic Acids Res. (1990). doi:https://doi.org/10.1093/nar/18.10.3091.

[47] K.J. Livak, T.D. Schmittgen, Analysis of relative gene expression data using real-time quantitative PCR and the $2-\Delta\Delta CT$ method, Methods. 25 (2001) 402–408, https://doi.org/10.1006/meth.2001.1262.